Quantum Electronics **38** (10) 895–902 (2008)

LASERS

PACS numbers: 42.55.Px; 42.60.By; 42.62.Eh; 42.62.Fi
DOI: 10.1070/QE2008v038n10ABEH013806

Semiconductor laser with the subhertz linewidth

A.N. Matveev, N.N. Kolachevsky, J. Alnis, T.W. Hänsch

Abstract. **A semiconductor laser emitting at 972 nm is stabilised with respect to a vibrationally and thermally compensated reference Fabry–Perot resonator with the vertical axis. The supporting points lie in the horizontal symmetry plane of the resonator, the influence of vibrations in the vertical direction being substantially suppressed in this case. This configuration provides a low sensitivity of the laser emission frequency to vertical accelerations of the reference resonator. To reduce the influence of temperature fluctuations, the resonator is made of an ULE (ultra-low-expansion) glass and is kept at temperature at which the expansion coefficient of this glass is close to zero. The laser linewidth is smaller than 0.5 Hz and the frequency drift is ~ 0.1 Hz s^{-1}. The minimum of the Allan deviation achieved for 3 s is 2×10^{-15}. The laser was used to record the spectra of the 1S–2S transition in atomic hydrogen.**

Keywords: *semiconductor laser, frequency stabilisation, subhertz spectral width.*

1. Introduction

Lasers emitting very narrow lines are required for the development of optical atomic clocks and applications in ultrahigh-resolution spectroscopy. To provide the high stability and accuracy of an optical clock (better than 10^{15}), a laser source should have the linewidth of ~ 1 Hz. During the past decade, a considerable progress has been achieved in the field of laser frequency stabilisation. More and more attention is being paid to the frequency stabilisation of semiconductor lasers, which have a simple design, a broad tuning range, and are low-cost. However, semiconductor lasers have the excessive noise caused by the amplitude–phase coupling, which complicates their stabilisation [1]. Thus, the linewidth of a semiconductor laser can achieve hundreds of megahertz [2]. The narrowing of the emission line of a semiconductor laser is usually performed in two stages: first by using the optical feedback from an external dispersion resonator, which allows the line narrowing to 1 kHz–1 MHz [3–5], and then by using an electronic feedback loop by the transmission peak of an external stable resonator [6–8]. Although the electronic stabilisation of the laser frequency with respect to the transmission peak of an external reference resonator with the subhertz mutual instability was demonstrated already in 1988 [9] (the laser emission frequency virtually coincides with the frequency of a resonator mode when the feedback loop operated properly), the development of resonators providing the subhertz stability level took ten more years. Until recently such systems were extremely inconvenient and were used only in a limited number of laser experiments performed in the leading laboratories of the world.

Our paper is devoted to the development of a compact reference resonator providing the subhertz linewidth of a 972-nm semiconductor laser. The fourth harmonic of this laser can be used to excite the two-photon 1S–2S transition with the natural width of 1.3 Hz in a hydrogen atom. The laser can be also employed in a number of other experiments, in particular, for studying the spectra of the 1S–2S transition in atomic tritium and antihydrogen [10]. To provide a narrow laser line, the distance between mirrors in the reference Fabry–Perot resonator should be extremely stable, which severely restricts the admissible levels of vibrations, temperature fluctuations, and fluctuations of the refractive index of a medium between the mirrors. Thus, to provide the linewidth 1 Hz of a laser stabilised with respect to the reference resonator of length 10 cm, fluctuations of the optical length of the resonator should not exceed 10^{-15} m.

The frequency stabilisation of a tunable laser at the subhertz level has been demonstrated for the first time in 1998 [11]. A dye laser was stabilised with respect to the reference resonator with a horizontal axis. The vibration isolation was achieved by suspending an optical table with rubber strips to the laboratory room ceiling. This provides a low intrinsic vibrational frequency of the system and suppression of adverse vibrations; however, the large mass and size of the system exclude the possibility of its transport.

An alternative approach is based on a new principle of mounting the reference resonator, which provides the

A.N. Matveev, N.N. Kolachevsky P.N. Lebedev Physics Institute, Russian Academy of Sciences, Leninsky prosp. 53, 119991 Moscow, Russia; Moscow Institute of Physics and Technology (State University), Institutskii per. 9, 141700 Dolgoprudnyi, Moscow region, Russia; e-mail: art_matan@mail.ru, kolachbox@mail.ru;
J. Alnis Max Planck Institute of Quantum Optics, Hans-Kopfermann-Str. 1, 85748 Garching, Germany; e-mail: Janis.Alnis@mpq.mpg.de;
T.W. Hänsch Max Planck Institute of Quantum Optics, Hans-Kopfermann-Str. 1, 85748 Garching, Germany; Ludwig-Maximilians University, Geschwister-Scholl-Platz 1, 80539 Munuch; e-mail: t.w.haensch@mpq.mpg.de

Received 29 January 2008; revision received 22 April 2008
Kvantovaya Elektronika **38** (10) 895–902 (2008)
Translated by M.N. Sapozhnikov

reduction of the assembly total mass down to 10 – 20 kg. In the new configuration, the supporting points of the Fabry–Perot resonator with the vertical axis lie in its horizontal symmetry plane. The vertical acceleration leads to almost symmetric expansion and compression of the upper and lower halves of the resonator, so that the distance between resonator mirrors remains virtually invariable due to the mutual compensation of expansion and compression [12]. The resonator should be mounted on rigid posts fixing its position with respect to a stage. This provides the suppression of the Doppler effect inherent in systems in which the resonator is suspended with threads or spring-mounted. As a stage, a commercial system with the active suppression of vibrations, manufactured, for example, by Halcyonics Inc., is used. In this case, the mechanical coupling of the resonator with the stage proves to be rather rigid. However, the high stability of the resonator itself and the system of active suppression of vibrations provide the sufficient suppression of both vertical and horizontal accelerations, which is required for obtaining subhertz linewidths. The high degree of stabilisation of resonators was also achieved by other research groups, which used resonators with the horizontal axis and supporting points lying in the horizontal symmetry plane [13].

To eliminate fluctuations of the refractive index, it is necessary to accommodate the resonator in a vacuum chamber where pressure fluctuations should not exceed 10^{-8} mbar. This requirement can be easily fulfilled by placing the resonator into a vacuum chamber evacuated with an ion-getter pump. However, an important problem in the development of highly stable resonators is temperature fluctuations of their length l. At present the best material used for manufacturing the body and mirrors of reference resonators operating at room temperatures is the ULE (ultra-low-expansion) Corning glass [14]. A specific feature of this material is the presence of the so-called zero point at which the thermal expansion coefficient of the material is zero. The detuning $\Delta\nu$ of the resonator frequency near the zero point depends quadratically on temperature:

$$\Delta\nu/\nu = \Delta l/l \approx 10^{-9}(T - T_{\rm cr})^2, \qquad (1)$$

where T is the resonator temperature and $T_{\rm cr}$ is the temperature at the zero point.

To reduce the influence of temperature fluctuations, it is desirable to stabilise the temperature of the Fabry–Perot resonator near $T_{\rm cr}$. In this case, the length instability will be caused by a slow recrystallisation of the ULE glass (thus, the relevant frequency for the resonator used in [15] was $\sim$65 mHz s^{-1}). Our measurements showed that the temperature $T_{\rm cr}$ for our ULE glass sample was $\sim$10 °C, which is noticeably lower than room temperature. The external cooling of a vacuum chamber is a complicated technical problem because of the condensation of moisture on input windows, and for this reason most of the existing resonators operate at temperatures considerably exceeding $T_{\rm cr}$.

In this paper, we used two systems to stabilise 972-nm semiconductor lasers. Both systems employed identical Fabry–Perot resonators FP1 and FP2; however, their temperature stabilisation systems were substantially different. The FP1 resonator was equipped with a heating system providing the temperature stabilisation near 31 °C, which is considerably higher than $T_{\rm cr}$. The temperature stabilisation system with heating, which will be described below, was successfully used in previous experiments [8, 15]. Another system, which was developed for the first time, provided the cooling of the FP2 resonator down to the temperature $T_{\rm cr}$ by using Peltier elements placed in vacuum. We describe below the design of devices and present the parameters of stabilised semiconductor lasers and the results of the study of the spectrum of the 1S – 2S transition in atomic hydrogen.

2. Experimental setup

Figure 1 shows the scheme of a vertical resonator used in our paper, which was manufactured by ATF Inc. [16]. Two mirrors are attached by optically contacting the resonator body of length 77.5 mm. The mirror substrates are also made of the ULE glass. The resonator body has the shape of a 'rugby ball' as approximation to the spherical shape providing the minimal excitation of vibrational modes. The reflectance of mirrors was $\sim$99.999 % at 972 nm. The multilayer reflecting structure contained 38 SiO_2 and Ta_2O_5 layers with a total thickness of $\sim$0.5 μm. One of the mirrors was plane and the other had the radius of curvature of 0.5 m. The resonator was mounted on three Teflon posts inserted into a ring made of Zerodur. The ring suppresses the influence of temperature on the distance between the posts and prevents the appearance of radial forces from posts on the resonator body. The posts had circular channels reducing their rigidity in the horizontal direction and weakening the influence of horizontal vibrations.

2.1 Temperature stabilisation system of the FP1 resonator

Figure 2 shows the temperature stabilisation system of the FP1 resonator. The resonator is located inside a cylindrical vacuum chamber made of duralumin. Due to the high heat

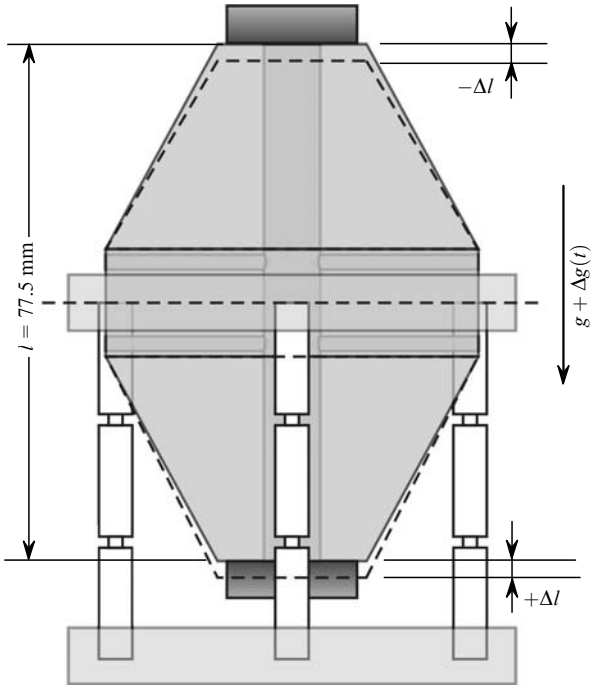

Figure 1. Scheme of the Fabry–Perot resonator with the vertical axis fixed in the horizontal symmetry axis. In the case vertical acceleration g, the compression of the upper half of the resonator is compensated by the elongation of its lower half, and the total resonator length remains constant.

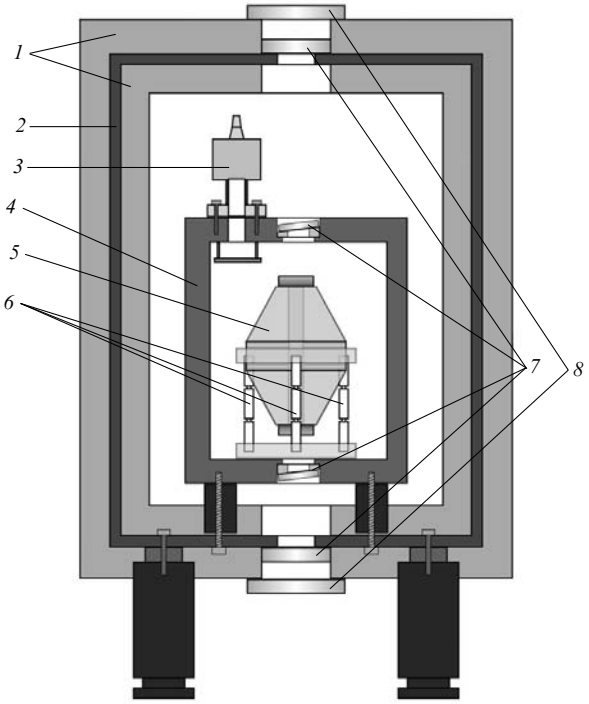

Figure 2. System for temperature stabilisation of the FP1 resonator: (*1*) polyurethane foam thermal isolation; (*2*) duralumin container (the first stage of temperature stabilisation); (*3*) ion-getter pump with capacity 3 L s^{-1}; (*4*) duralumin vacuum chamber; (*5*) vertical-axis resonator; (*6*) Teflon rods; (*7*) windows of the vacuum chamber and the first stabilisation stage; (*8*) interference filters.

conduction, the aluminium chamber provides a more uniform temperature distribution than stainless steel chambers. Duralumin was subjected to chemical processing (passivation), which allowed us to evacuate the chamber down to 10^{-7} mbar by using an ion-getter pump with a capacity of 3 L s^{-1}. All the vacuum seals were provided by using a indium wire.

The temperature of the vacuum chamber was stabilised with the help of a heater and an electronic proportionally integrating (PI) feedback circuit. The system stabilises temperature at 30.5 °C only at the location site of a temperature sensor, not monitoring fluctuations and temperature gradients at the other sites of the surface. To reduce the influence of temperature gradients and suppress heat exchange with the environment, the second, external six-cannel stabilisation system is used. The vacuum chamber is placed into a container made of heat conducting duralumin plates, each of them being independently heated and stabilised with the help of a fast relay two-position controller providing the temperature stability at the sensor site no worse than 100 mK. The second stage produces the uniform thermal background with temperature 30 °C around the vacuum chamber with minimal temperature gradients and drifts. Both the vacuum chamber and duralumin container are covered with a thermal insulation layer for passive suppression of temperature oscillations. The uniform distribution of the thermal power was provided by using thin-film heating elements. The AD590 sensors (Analog Devices, USA) used in temperature control feedback systems were preliminarily calibrated. The heat exchange time constant of the resonator was ~3 h.

The temperature stabilisation system provides the temperature stability of the external surface of the vacuum chamber ~1 mK during ten hours and ~5 mK for a week, which was measured with an independent sensor. The residual temperature fluctuations are caused by fluctuations of room temperature and the influence of these fluctuations on temperature controllers themselves. Thus, the temperature of the PI controller also was stabilised with an accuracy of 0.1 K to prevent a drift caused by the influence of temperature on the capacity of the capacitors (ten foil 22-μF capacitors), the resistance of the resistors, and the bias voltage of semiconductor elements.

2.2 Temperature stabilisation system of the FP2 resonator

To provide the efficient cooling of the resonator together with maintaining the ultimately stable temperature, we used a new construction shown in Fig. 3. The reference resonator was located inside two duralumin tubes with 5-mm-thick walls, which were cooled with Peltier elements. The tubes were placed into a vacuum stainless steel chamber, which simultaneously served as a temperature buffer cooling the external (heating) side of a Peltier element. The use of two tubes reduced the inhomogeneity of the thermal background and provided good thermal isolation of the resonator. The external tube was cooled with a Peltier element of size 50×50 mm down to the zero-point temperature of the resonator $T_{cr} = 12.5\,^{\circ}C$ (see below). The temperature of the inner tube was stabilised with a second Peltier element of size 20×20 mm also near T_{cr}. Temperature sensors included into the corresponding feedback circuits were glued to the surfaces of tubes near the corresponding Peltier elements. An additional temperature sensor for independent temperature control was glued to the surface of the inner tube at a large distance from Peltier elements. Feedback systems stabilising the temperature of both casings are usual PI controllers, which are also used to stabilise the temperature of semiconductor lasers.

The temperature of the walls of the vacuum chamber itself was not controlled and achieved 34 °C. Vacuum was

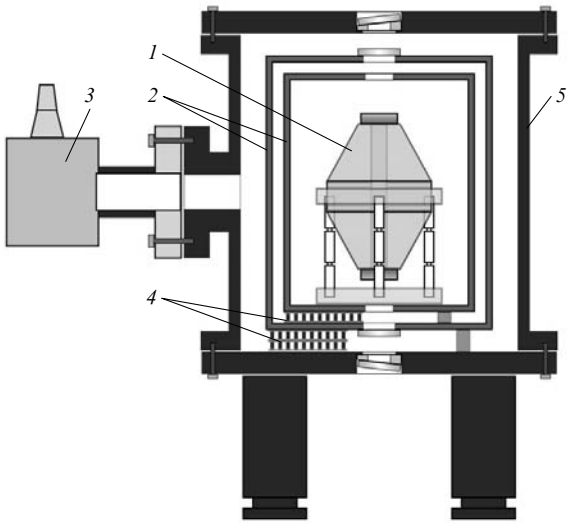

Figure 3. System for temperature stabilisation of the FP2 resonator: (*1*) vertical-axis resonator; (*2*) duralumin tubes; (*3*) ion-getter pump with capacity 20 L s^{-1}; (*4*) Peltier elements; (*5*) vacuum chamber.

maintained by using an ion-getter pump with capacity 20 L s^{-1}. The measurements of temperature fluctuations of the inner casing performed with the independent sensor showed that the typical temperature instability was ~ 15 mK during several days, which is approximately three times worse than the stability achieved for the FP1 resonator. Nevertheless, the long-term stability of the resonator frequency was improved approximately by two orders of magnitude due to approach to the zero point of the ULE glass [see expression (1)]. During several first weeks after evacuation of the chamber, a few abrupt temperature jumps amounting to several millikelvin were observed, which are probably caused by transient processes in Peltier elements.

2.3 Frequency stabilisation of a semiconductor laser with respect to the Fabry–Perot resonator frequency

Both vacuum chambers with resonators and temperature stabilisation systems were mounted on two stages of size 40×40 cm providing the active suppression of vibrations. Due to the use of the vertical resonator, the size and weight of the system were considerably reduced compared to the system employed earlier for studying the hydrogen spectrum [15]. The resonators were used to stabilise two almost identical 972-nm diode lasers with external resonators in the Littrow mounting.

The optical scheme used to stabilise lasers is shown in Fig. 4. Laser radiation is delivered through a single-mode fibre to the stage with the reference resonator. The phase and intensity noises introduced by the fibre were compensated by using a standard active compensation system with an acousto-optic modulator [17]. The Gaussian mode at the fibre output is matched with the resonator mode with the help of a lens ($f = 500$ mm). The laser frequency is stabilised by the frequency of a certain resonator mode by the Pound–Drever–Hall (PDH) method [14]. This method of laser frequency stabilisation is based on the active locking of the laser radiation phase to the phase of a wave in the resonator averaged due to the long lifetime of a photon in the resonator [18]. In this case, the resonator operates as a flywheel, by filtering rapid phase fluctuations of input radiation. Due to the active phase locking, a laser with the natural linewidth of ~ 1 MHz stabilised with respect to the transmission peak of the resonator of width 7 kHz emits a narrow line with the subhertz width.

A number of reasons leading to the zero-level shift in the PDH locking scheme considerably affect the laser frequency stability. One of the important undesirable factors is the amplitude modulation of the field accompanying the phase modulation in the PDH locking scheme. This effect is very strong if the phase modulation is provided by modulating the diode current. Because of this, we used a scheme in which modulation was performed by an external electro-optical modulator and the polarisation of light was chosen to provide the minimal amplitude modulation. In addition, to reduce the drift of optical axes of crystals, the temperature of the electrooptical modulator was stabilised with an accuracy of 0.1 K. The locking zero can be also shifted due to interference effects, which were eliminated by placing an optical isolator in front of the fibre.

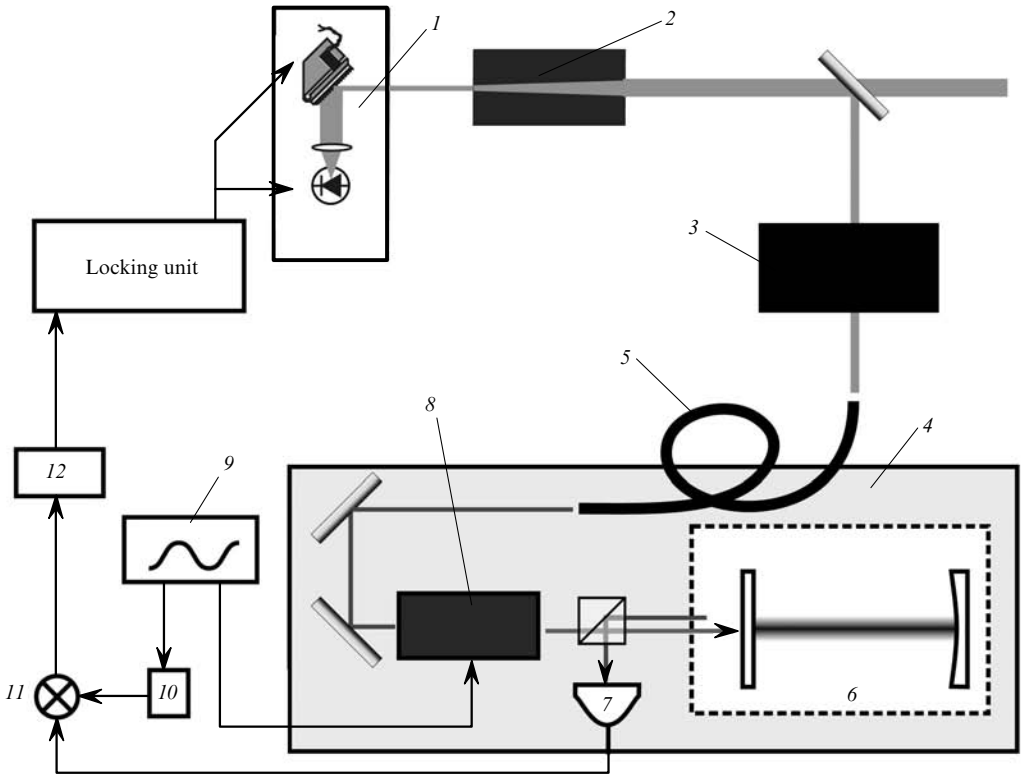

Figure 4. Scheme of the diode laser frequency stabilisation by the Pound–Drever–Hall method: (*1*) external cavity diode laser; (*2*) tapered amplifier; (*3*) acousto-optic modulator; (*4*) active vibration suppression stage; (*5*) optical fibre; (*6*) reference resonator; (*7*) photodiode; (*8*) electrooptical modulator operating in the phase modulation regime; (*9*) radiofrequency generator; (*10*) phase shifter; (*11*) balance mixer; (*12*) low-frequency filter; the optical fibre is equipped with a noise-compensation system, which, as matching optics, is not shown in the figure.

The laser frequency was controlled, as usual, by employing two channels – the fast channel (controlling the laser diode current) and the slow channel (controlling the rotation of a diffraction grating with the help of a piezoelectric element). The frequency curve of a proportionally integro-differential controller of the laser frequency provided a high amplification (more than 60 dB) at low frequencies and the bandwidth of up to 10 MHz.

The optimal operation of the locking scheme was achieved by coupling the radiation power ~ 20 μW into the resonator. The increase in the radiation power resulted in the noticeable influence of radiation intensity fluctuations on the resonator frequency, which was characterised by the value 5 Hz mW^{-1}. The decrease in the radiation power reduced the signal-to-noise ratio of photodetectors (silicon pin-photodiodes) and impaired the frequency stability.

3. Experimental results

3.1 Parameters of the FP1 and FP2 resonators

The finesse of the resonators determined from the radiation decay time was 4.1×10^5 and 4.0×10^5 for the FP1 and FP2 resonators, respectively. The temperature at the zero point was determined from the dependence of the beat frequency of two laser fields on the temperature of one of the resonators (Fig. 5). For this purpose, the temperature of one of the resonators was kept constant, while the temperature of the other was varied, the temperature of the resonator under study being stabilised for ~ 24 hours. After cessation of transient processes, the beat frequency of the light fields was measured and the results were approximated by quadratic function (1). Its minimum corresponded to the zero point of the resonator. The temperatures T_{cr} measured for the FP1 and FP2 resonators were 7 ± 2 °C and 12.5 ± 0.1 °C, respectively. These values are different most likely due to the influence of posts and residual stresses in resonators.

A simple estimate shows that the cooling of the resonator down to the temperature T_{cr} considerably reduces its sensitivity to temperature fluctuations. By assuming that the temperature adjustment accuracy is 0.1 °C, we obtain the sensitivity of the FP1 resonator equal approximately to 10 kHz mK^{-1}, whereas the sensitivity of the FP2 resonator is reduced to 50 Hz mK^{-1}. Note that the contribution of the temperature expansion of the multilayer coating of mirrors for the FP2 resonator is considerable and is equal to 20 Hz mK^{-1}. Rapid temperature fluctuations of the environment (heat exchange mainly occurs due to radiation) affect first of all the relatively thin mirror substrates and the multilayer coating, which is followed by thermalisation with the resonator body. This means that the real sensitivity of the resonator to rapid temperature fluctuations can considerably exceed the estimate even in the case of its stabilisation near T_{cr}. This effect was observed in experiments. Thus, even when the zero point of the ULE glass is used, the resonator temperature should be stabilised with the maximum possible accuracy.

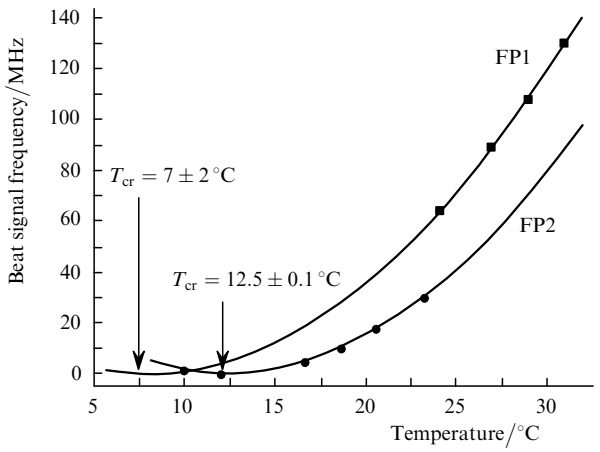

Figure 5. Determination of the zero point of the FP1 and FP2 resonators (see text).

3.2 Residual phase noise of a semiconductor laser

The study of the beat signal of light fields from stabilised lasers with the help of a spectrum analyser showed that, apart from a narrow spectral peak containing the main part of the signal, the high-frequency noise forming a pedestal of width of several megahertz was also observed (Fig. 6). This high-frequency noise appears due to the residual phase noise of a semiconductor laser, which is not completely compensated by the feedback. The optimisation of the feedback parameters reduces the noise pedestal, but does not suppress it completely.

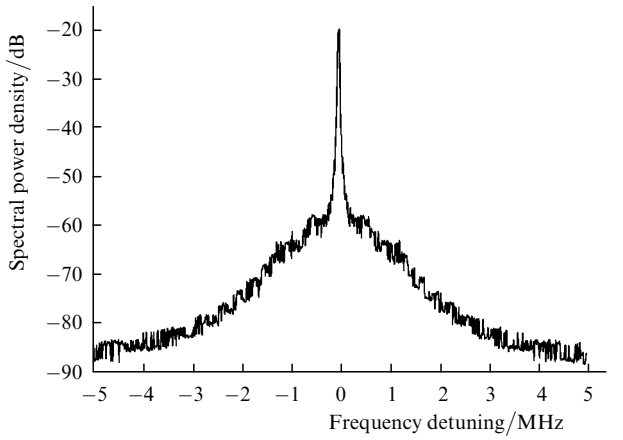

Figure 6. Spectrum of the beat signal of light fields of two laser systems at 972 nm. The noise pedestal is caused by the phase noise. The resolution of the spectrum analyser is 20 kHz.

The measurements showed that when 20 μW of radiation power was coupled into the reference resonator (operating regime), the central peak corresponding to the carrier frequency contained $99.0\% \pm 0.1\%$ of the total power. An increase in the power used for locking leads to the increase in this value. Thus, for example, when 200 μW of laser radiation power was coupled into the resonator, the power fraction at the carrier frequency increased up to $99.7\% \pm 0.1\%$. However, such an operation regime is unfavourable from the point of view of the spectral width of the central peak (see above). The noise pedestal poses a serious problem in the spectroscopy of the 1S–2S transition in the hydrogen atom because its excitation involves three two-photon processes. The frequency multiplication leads to the increase in the phase noise, the decrease in the power fraction at the carrier frequency, and reduces the transition excitation efficiency [19].

3.3 Frequency drift in resonators and the Allan deviation

The beat signal of laser fields was heterodyned in the region near 10 MHz and transmitted through a band-pass filter of width 1 MHz. Figure 7a shows the frequency drift of the beat signal during half an hour. The average frequency drift is several tens of millihertz per second (for the realisation presented in Fig. 7a, this drift is 15 mHz s^{-1}), whereas the maximum drift does not exceed 1 Hz s^{-1}, remaining usually within ± 100 mHz s^{-1} (the drift magnitude depends on the operation reliability of a laboratory climate control system). Unfortunately, it is impossible in this case to determine which of the resonators makes the greater contribution to the observed frequency drift. The FP1 resonator is better isolated and slower responses to temperature variations in the environment, but it is highly sensitive to temperature fluctuations (10 kHz mK^{-1}). The FP2 resonator is worse isolated from the environment because the vacuum chamber serves as a thermal radiator, however, it has a considerably lower temperature sensitivity (50 Hz mK^{-1}). At present we plan to measure the absolute radiation frequency of stabilised semiconductor lasers with respect to the hydrogen maser frequency by using a femtosecond frequency comb [20].

The Allan deviation corresponding to data in Fig. 7a is presented in Fig. 7b. The deviation achieves the minimum (2×10^{-15}) for the averaging time 3 s. This is only twice as large as the theoretical limit caused by the thermal noise of the resonator [21].

3.4 Spectral linewidth

The linewidth was measured by heterodyning the beat signal in the 100-Hz region, which allowed us to study the carrier spectrum by using a Fourier spectrum analyser. The recording time of one data realisation was 4 s, which corresponds to the resolution of the spectrum analyser equal to 0.25 Hz. For twelve successively recorded realisations, the spectral width of the peak varied from 0.3 to 0.75 Hz, which gave 0.47 ± 0.14 Hz after averaging. Figure 8 presents the result of averaging of the obtained lines after combining their centres (compensation of the laser frequency drift). The spectral line profile is well approximated by a Lorentzian.

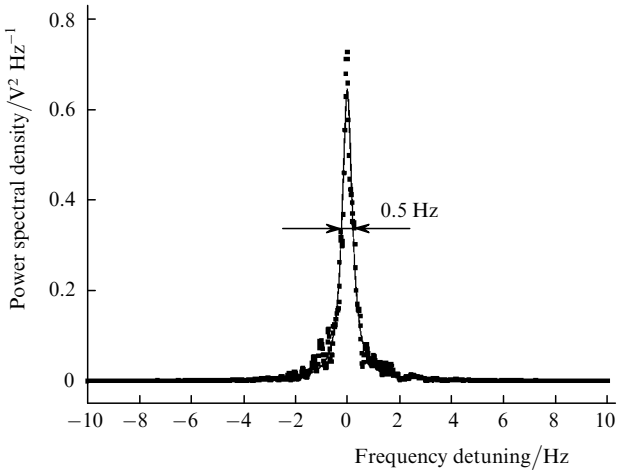

Figure 8. Spectrum of the beat signal of two laser systems at 972 nm obtained with a Fourier spectrum analyser. The resolution of the spectrum analyser is 0.25 Hz.

The beat signal was also recorded by using a standard digital oscilloscope. The typical oscillogram obtained after the filtration of high frequencies looks like a sinusoid with a slowly fluctuating frequency (Fig. 9). The heterodyning of the beat signal to the sound frequency region followed by its monitoring with a dynamic loudspeaker is convenient to use for the adjustment of the system and determining the factors affecting the frequency stability of the laser system.

4. The 1S – 2S transition spectrum of the hydrogen atom

By using a laser stabilised with respect to the FP1 resonator, we recorded the 1S – 2S transition spectra of the hydrogen atom. For this purpose, laser radiation was

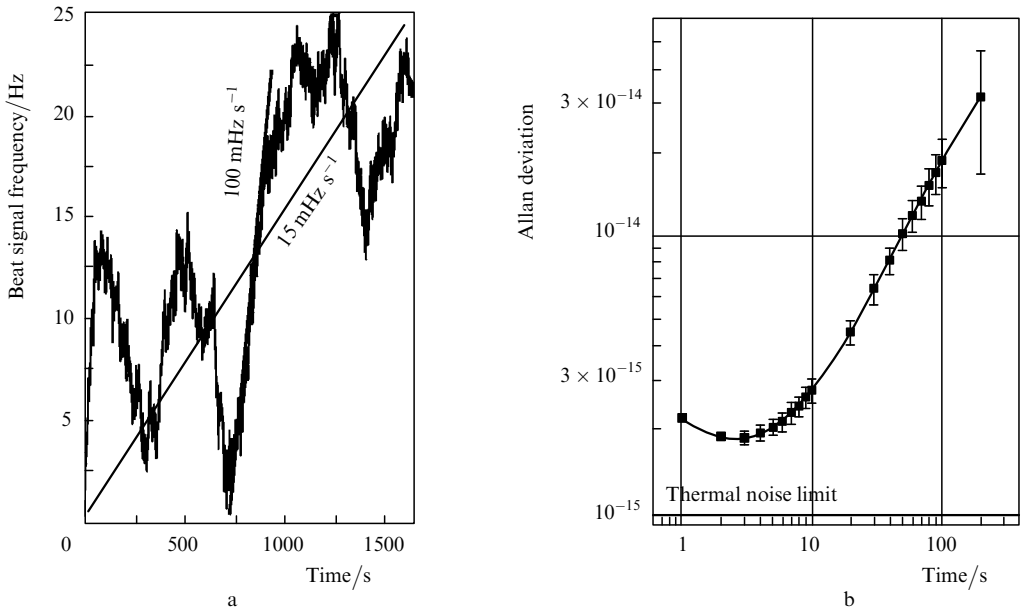

Figure 7. Drift of the beat signal frequency of light fields of two laser systems (a) and the corresponding Allan deviation (b).

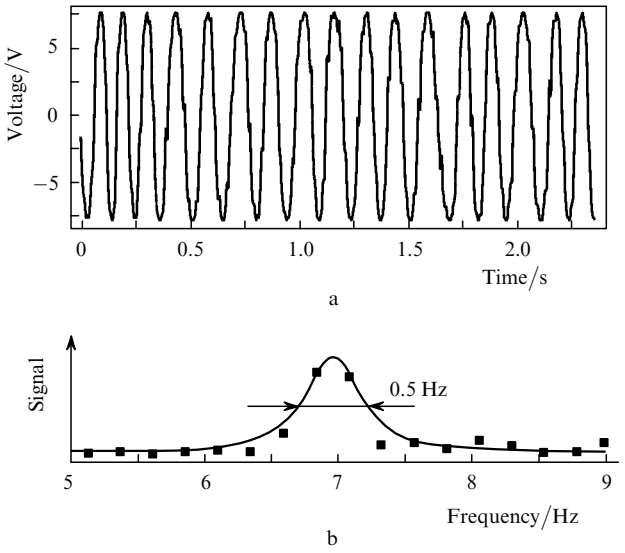

Figure 9. Beat signal of two laser systems at 972 nm recorded with a digital oscilloscope (a) and the spectrum obtained by the Fourier transform of this signal (b). The result is consistent with observations obtained by using a Fourier spectrum analyser.

amplified in a tapered amplifier providing 650 mW of output power and was directed to two successive stages for second harmonic generation [8]. The second stage generated ~ 5 mW of output power at 243 nm, which was required for studying the two-photon spectra of atomic hydrogen. The spectra were recorded by tuning the laser frequency with the help of the acousto-optic modulator operating in the double-pass regime. Atomic hydrogen was excited in a cold beam (the temperature of hydrogen atoms was 5–7 K) inside a linear resonator, which increased the radiation power density and provided Doppler-free excitation in counterpropagating beams. Hydrogen atoms in the 2S state were detected with a photomultiplier which counted photons at 121 nm appearing due to the decay of excited hydrogen atoms to the ground state in a weak electric field.

Figure 10 shows the typical 1S–2S transition spectrum. The spectroscopic method used in the paper allows us to obtain signals both from all the atoms of the total Maxwell distribution and from groups of atoms with low velocities. The velocity selection is performed by the time-of-flight method and reduces the contributions of the time-of-flight broadening and second-order Doppler effect [15]. By using vertical reference resonators to stabilise a semiconductor laser, we have managed to record considerably narrower resonances compared to these obtained in [8]. The estimates show that the excitation efficiency did not exceed 50 %, which is related to the residual noise of the semiconductor laser. The spectral resolution of the setup was ~ 4 kHz (calculated for $\lambda = 121$ nm).

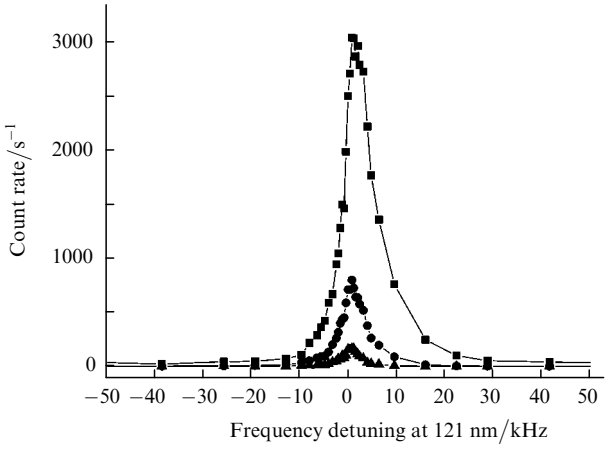

Figure 10. The 1S–2S transitions lines in atomic hydrogen obtained with the help of the laser system with the FP1 resonator from all the atoms of the total Maxwell distribution (■) and from groups of atoms with velocities smaller than 620 m s^{-1} (●) and smaller than 310 m s^{-1} (▲).

5. Conclusions

We have developed two independent laser setups based on 972-nm semiconductor lasers stabilised with respect to reference Fabry–Perot resonators with vertical axes. The reference resonator design insensitive to vibrations provided the laser linewidth smaller than 0.5 Hz. We have used a new method for cooling the reference resonator down to the temperature corresponding to the zero point of the ULE glass, which considerably improved the stability of the resonator frequency at large time intervals. The frequency drift of the laser systems was ~ 0.1 Hz s^{-1}. A small size of the resonator allowed us to achieve the high temperature stability. The Allan deviation for the frequency beats of the fields of stabilised laser systems achieves 2×10^{-15} for 3 s. The power fraction at the carrier frequency is 99 %, which allows the investigation of the 1S–2S transition spectrum of the hydrogen atom with the efficiency of ~ 50 %. It has been shown that these laser systems can be used to excite the narrow 1S–2S transition spectra with the resolution 4 kHz (calculated for $\lambda = 121$ nm). The laser system is compact and can be easily transported to other laboratories for performing experiments with exotic hydrogen-like systems.

Acknowledgements. This work was partially supported by the Russian Foundation for Basic Research (Grant No. 08-07-00127a), Grant MD-887.2008.2 of the President of the Russian Federation, the Foundation for Assistance to the Russian Science, and the Alexander Humboldt Foundation.

References

1. Henry C. *IEEE J. Quantum Electron.*, **18**, 259 (1982).
2. Bogatov A.P., Eliseev P.G., Sverdlov P.N. *Kvantovaya Elektron.*, **1**, 2286 (1974) [*Sov. J. Quantum Electron.*, **4**, 1275 (1974)].
3. Belenov E.M., Velichansky V.L., Zibrov A.S., Nikitin V.V., Sautenkov V.A., Uskov A.V. *Kvantovaya Elektron.*, **10**, 1232 (1983) [*Sov. J. Quantum Electron.*, **13**, 792 (1983)].
4. Akul'shin A.M., Basov N.G., Velichansky V.L., Zibrov A.S., Zverkov M.V., Nikitin V.V., Okhotnikov O.G., Senkov N.V., Sautenkov V.A., Tyurikov D.A., Yurkin E.K. *Kvantovaya Elektron.*, **10**, 1527 (1983) [*Sov. J. Quantum Electron.*, **13**, 1003 (1983)].
5. Dahmani B., Hollberg L., Drullinger R. *Opt. Lett.*, **12**, 876 (1987).
6. Stoehr H., Mensing F., Helmcke J., Sterr U. *Opt. Lett.*, **31**, 736 (2006).
7. Ludlow A.D., Huang X., Notcutt M., Zanon-Willette T., Foreman S.M., Boyd M.M., Blatt S., Ye J. *Opt. Lett.*, **32**, 641 (2007).
8. Kolachevsky N., Alnis J., Bergeson S.D., Hänsch T.W. *Phys. Rev. A*, **73**, 021801 (2006).

9. Salomon C., Hils D., Hall J.L. *J. Opt. Soc. Am. B*, **5**, 1576 (1988).
10. Gabrielse G., Bowden N.S., Oxley P., Speck A., Storry C.H., Tan J.N., Wessels M., Grzonka D., Oelert W., Schepers G., Sefzick T., Walz J., Pittner H., Hänsch T.W., Hessels E.A. *Phys. Rev. Lett.*, **89**, 213401 (2002).
11. Young B.C., Cruz F.C., Itano W.M., Bergquist J.C. *Phys. Rev. Lett.*, **82**, 3799 (1999).
12. Notcutt M., Ma L.-S., Ye J., Hall J.L. *Opt. Lett.*, **30**, 1815 (2005).
13. Nazarova T., Riehle F., Sterr U. *Appl. Phys. B*, **83**, 531 (2006).
14. http://www.corning.com/specialtymaterials.
15. Fischer M., Kolachevsky N., Zimmermann M., Holzwarth R., Udem Th., Hänsch T.W., Abgrall M., Grünert J., Maksimovic I., Bize S., Marion H., Pereira Dos Santos F., Lemonde P., Santarelli G., Laurent P., Clairon A., Salomon C., Haas M., Jentschura U.D., Keitel C.H. *Phys. Rev. Lett.*, **92**, 230802 (2004).
16. http://www.atfilminc.com.
17. Ma L.-S., Jungner P., Ye J., Hall J.L. *Opt. Lett.*, **19**, 1777 (1994).
18. Drever R.W.P., Hall J.L., Kowalski F.V., Hough J., Ford G.M., Munley A.J., Ward H. *Appl. Phys.*, **31**, 97 (1983).
19. Matveev A.N., Kolachevsky N.N., Alnis J., Hänsch T.W. *Kvantovaya Elektron.*, **38**, 391 (2008) [*Quantum Electron.*, **38**, 391 (2008)].
20. Reichert J., Holzwarth R., Udem Th., Hänsch T.W. *Opt. Commun.*, **172**, 59 (1999).
21. Notcutt M., Ma L.-S., Ludlow A.D., Foreman S.M., Ye J., Hall J.L. *Phys. Rev. A*, **73**, 031804 (2006).